Geoderma 285 (2017) 260–269

Contents lists available at ScienceDirect

Geoderma

journal homepage: www.elsevier.com/locate/geoderma

Combined soil-terrain stratification for characterizing catchment-scale soil moisture variation

Doug Baldwin [a], Kusum J. Naithani [b], Henry Lin [c,*]

[a] Department of Geography, The Pennsylvania State University, University Park, PA, 16802, USA
[b] Department of Biological Sciences, University of Arkansas, Fayetteville, AR, 72701, USA
[c] Department of Ecosystem Science and Management, The Pennsylvania State University, University Park, PA, 16802, USA

ARTICLE INFO

Article history:
Received 29 April 2015
Received in revised form 8 September 2016
Accepted 25 September 2016
Available online 17 October 2016

Keywords:
Soil moisture
Catchment hydrology
Catchment stratification
Terrain attributes
Soil type

ABSTRACT

Soil properties and terrain characteristics influence spatiotemporal patterns of soil moisture across a watershed. To improve the predictive power of landscape hydrologic models, it is essential to consider both soil and terrain attributes when stratifying a catchment into similar hydrologic functional units. In this study, we developed and validated a new catchment-scale stratification scheme for the Shale Hills watershed by combining soil and terrain attributes in an attempt to delineate soil-landscape units with similar soil moisture dynamics. Terrain was combined with soils information by first using a Random Forest supervised classification algorithm to predict a detailed soil map using 47 field soil samples and terrain variables derived from 1-m LiDAR. A slope class map generated from the LiDAR-derived digital elevation model (DEM) was overlaid on the predicted soil map to delineate areas of similar slope value across the catchment. We compared the performance of this new stratification scheme with two classical stratification schemes, a soil map developed from detailed field survey and a landform unit map based on the DEM, for estimating soil moisture time-series across the forested watershed. The combined soil-terrain method outperformed classical stratification schemes in estimating soil moisture time-series over a 4-year period. Our results demonstrate that combining soil and terrain attributes can help improve the stratification of a catchment into similar soil hydrologic functional units, which is valuable to distributed hydrology modeling and other applications.

1. Introduction

Understanding the link between soil moisture patterns and landscape features is critical to improving landscape hydrologic modeling (Band et al., 1993; Pauwels et al., 2001; Yu et al., 2014). A common assumption in catchment hydrology is that terrain places a dominant control on hydrologic functions (Beven and Kirkby, 1979; Winter, 2001). This assumption leads many researchers to parameterize hydrologic models based on landforms or sub-catchment units using terrain alone. Since topographic information in the form of digital elevation models (DEM) has been increasingly available, stratifying catchments into similar hydrologic functioning units with terrain has been widespread (Moore et al., 1991; Blöschl and Sivapalan, 1995; Winter, 2001). However, field-based soil properties are often not directly included in these stratification schemes, and terrain is assumed to be a proxy for inferring soil properties. These assumptions remain largely unchallenged, since many catchment hydrologic studies do not validate terrain-based sub-catchment units using *in situ* collected soil moisture data or compare model performance with actual soil distributions.

Topographically-based stratification approaches have been continuously improved over time with advancements in GIS and remote sensing technologies. Following the conceptual work by Beven and Kirkby (1979) and Dooge (1986), hydrologic response units (HRUs) have been developed by dividing a catchment into units of similar topography (Leavesley and Stannard, 1990). Park and van de Giesen (2004) used topographic variables (surface curvature and upslope contributing area) derived from DEM to stratify the Terrawarra Catchment and validated their landform units with a general linear modeling approach using *in situ* soil moisture measurements. Gharari et al. (2011) used a terrain-based index, called height above nearest drainage, along with slope value to stratify a catchment in Luxembourg into similar hydrologic functioning units.

Soil properties may have even higher correlations with catchment-wide soil moisture measurements than terrain variables, as Gomez-Plaza et al. (2001) have shown, where sand content was the most correlated variable with soil moisture content for both wet and dry conditions in semi-arid Spain. This suggests that combining soil and terrain attributes within a single stratification would be better for predicting catchment-scale soil moisture dynamics. Temporal patterns of soil moisture have been assessed with terrain and soil characteristics across a watershed (Canton et al., 2004) and some terrain variables are more related to the temporal structure of soil moisture patterns than others.

* Corresponding author.
E-mail address: henyrlin@psu.edu (H. Lin).

http://dx.doi.org/10.1016/j.geoderma.2016.09.031
0016-7061/

Given this finding, an analysis that addresses how well different terrain variables represent spatio-temporal patterns of soil moisture would be beneficial to any combined soil and terrain stratification study.

There is evidence that combining soil and terrain attributes can further improve catchment hydrologic stratifications (Lin et al., 2006). Takagi and Lin (2012) found that field soil moisture content was highly correlated with terrain variables, depth to bedrock, and clay content in the forested Shale Hills catchment at multiple depths, indicating that both soil and terrain properties are important attributes for defining sub-catchment units with similar soil hydrologic function. Devito et al. (2005) refined existing HRU boundaries by including information about soil texture and peatland cover, which improved catchment water flow predictions. Although a stratification that combines soil and terrain attributes is likely to better characterize catchment-scale soil moisture patterns, a combined soil-terrain stratification in predicting soil moisture patterns has yet to be developed and validated using *in situ* soil moisture data.

Given the importance of catchment stratification for scaling soil moisture and parameterizing distributed hydrologic models and the relative scarcity of the validation and comparison of different stratification methods with catchment-wide *in situ* soil moisture measurements, our objectives in this study are to: (1) uncover terrain variables that are significantly correlated with temporal structure of soil moisture across a catchment, and (2) compare the skill of a newly developed soil-terrain stratification scheme with two classical stratification schemes in predicting catchment-wide soil moisture with *in situ* data.

2. Materials and methods

2.1. Study site

The Shale Hills Catchment is a 7.9-ha forested watershed characterized by steep slopes (ranging from 25 to 48%) and narrow ridges, with elevation ranging from 256 to 310 m. The catchment valley is oriented in an east–west direction, which divides the catchment into two almost true north- and south-facing hillslopes. Several species of maple (*Acer* spp.), oak (*Quercus* spp.), and hickory (*Carya* spp.) are typical deciduous trees found on the sloping areas and on the ridges, while the valley floor is dominated by eastern hemlock (*Tsuga canadensis Carriére*) (Lin, 2006; Naithani et al., 2013). Oaks species are spread throughout the hillslope area, while maples and hickory are mostly situated on the south-facing slope. The climate at the Shale Hills is typical of humid temperate region, with long-term (>100 yr) mean monthly temperatures reaching a minimum of −3 °C in January and a maximum of 22 °C in July. Annual precipitation is about 980 mm (National Weather Service, State College, PA), with the majority of precipitation falling as rain during the spring through fall months (about 70–100 mm/month) and as snow in the winter (about 70 mm/month).

The soils at the Shale Hills were formed from Silurian-age shale residuum and colluvium. The soils are generally silt loams and silty clay loams in texture, with some clay loams and sandy clay loams. All soil types have an approximately 0.05 m thick litter layer (Oe horizon) due to the presence of forested cover over the entire catchment. The catchment is underlain by >200 m thick Rose Hill shale, a Silurian formation frequently associated with the iron-rich Clinton Ore. Many gravelly shale fragments (2–150 mm) are found throughout soil profiles, and the near surface shale is characterized as fractured bedrock.

2.2. Soil moisture monitoring

Volumetric soil water content (hereafter, “soil moisture”; unit: $cm^3\ cm^{-3}$) was collected manually at a weekly to bi-weekly interval from 106 sites (varied from 46 to 106 sites depending on weather and available field assistants) during 2007–2010. Soils were drilled down to 1.1 m or the beginning of bedrock (whichever is shallower), so that 5.1 cm diameter Schedule 40 PVC tubes could be installed vertically into the soil. During each data collection period, soil moisture was recorded at up to six depths (10, 20, 40, 60, 80, 100 cm) using a TRIME-FM Time Domain Reflectometry (TDR) probe (IMKO, Germany), which was inserted within the PVC access tube at each site. Site locations are distributed across the entire catchment (Fig. 1) representing all soil types and landforms and were chosen based on the field surveyed soil map. A total of 17,464 moisture measurements (Weikert = 5221, Berks = 3446, Rushtown = 4601, Blairton = 1345, and Ernest = 2851) recorded from 2007 to 2010 were used in this study.

2.3. Field surveyed soil map

The Hydropedology group at Penn State conducted a detailed soil survey throughout the catchment in cooperation with the USDA Natural Resources Conversation Services personnel (see Lin et al., 2006 for details). Transects were placed 50 m apart and aligned perpendicularly to the catchment's bedrock southwest to northeast orientation. During the survey, a total of 289 samples were taken, and five soil types were identified in the catchment. Soil thickness, landscape position, and depth to redoximorphic features were the main criteria used to differentiate these soil types.

The Weikert (loamy-skeletal, mixed, active, mesic Lithic Dystrudept) is the predominant soil type in the catchment, comprising 78% of the catchment, and is characterized as a thin soil on hilltops, planar, and convex hillslopes. The Rushtown (loamy-skeletal, over fragmental, mixed, mesic Typic Dystrochrept) is mostly located in the center of four dominant concave hillslopes and a large portion of the upper 100 m of the catchment valley. The Berks soil type (loamy-skeletal, mixed, active, mesic Typic Dystrudept) is well drained and largely distributed along the slope transitional zones between the shallow Weikert and the deep Rushtown soils. The Blairton soil type (fine-loamy, mixed, active, mesic Aquic Hapludult) is located in the valley bottom, with an argillic horizon at 0.2–0.8 m depth and few (2–5%) redox features starting at 0.8–1.1 m depth. The Ernest soil type (fine-loamy, mixed, superactive, mesic Aquic Fragiudults) is a very deep (>3 m depth to bedrock), poorly to moderately well-drained soil on the valley floor around the first-order stream with many redox features and a fragipan-like layer starting at 0.3–0.5 m depth.

2.4. Digital terrain, depth to bedrock, and landform units

A LiDAR flyover in February 2011 was used to generate a high-resolution 1 × 1 m DEM raster dataset for the Shale Hills. During pre-processing, TerraScan software (Terrasolid) classified raw LiDAR point data and ground points were interpolated across space using ordinary kriging (Guo and Si, 2008). A Gaussian filter was applied with a 4.5 × 4.5 m smoothing window to reduce noise in the DEM. Topographic variables derived from the LiDAR DEM included local slope value (Fig. 2a), vertical distance to stream (VDS, Fig. 2c; Olaya and Conrad, 2009), upslope contributing area (Fig. 2d; Tarboton, 1997), topographic wetness index (TWI, Fig. 2e; Beven and Kirkby, 1979), and surface curvature (Fig. 2f; Zevenbergen and Thorne, 1987) using SAGA GIS (Conrad et al., 2015). Local slope value [$m\ m^{-1}$], upslope contributing area [m^2], surface curvature [−], and TWI [−] were developed using the Basic Terrain Analysis module, and VDS [m] was calculated with the Vertical Distance to Channel Network module.

A depth to bedrock map (Fig. 2b) was obtained from catchment-wide auger sampling. A total of 318 auger data points were used in a regression kriging (Isaaks and Srivastava, 1989; Odeh et al., 1995) to interpolate depth to bedrock across the catchment. During the regression kriging, a backwards-stepwise algorithm (Venables and Ripley, 2002) was used to select a multiple linear regression model with DEM-derived terrain variables as covariates. The regression with the lowest Akaike's Information Criterion (AIC) was selected for regression kriging. The best multiple linear regression model contained surface curvature ($p = 0.008$) and TWI ($p < 0.001$) as covariates.

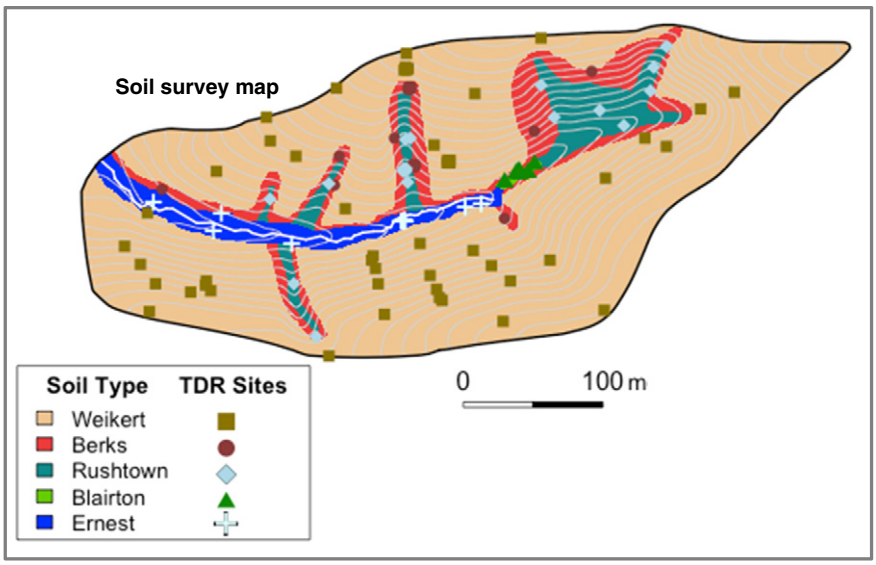

Fig. 1. Map of soil types (soil series) across the Shale Hills catchment based on detailed field soil survey. Locations with soil moisture data collection (TDR sites) are shown with symbols corresponding to different soil types. The stream is shown in white, and 3-m elevation contours are shown in light grey.

Park and van de Giesen (2004) developed a stratification method that uses terrain information alone for defining landform units and they validated it with field soil moisture data. We implemented this landform unit stratification method to generate landform units for the Shale Hills by using the relationship between surface curvature and log-transformed upslope contributing area derived from LiDAR. Variables used in this stratification method are shown in Table 2. It should be noted that Park and Van de Giesen gave planar hillslopes a threshold curvature values of 1 and -1, which correspond to 0.01 and -0.01 values for the surface curvature in the Shale Hills that were calculated using second-degree polynomial curvature algorithm (Zevenbergen and Thorne, 1987). (See Table 1.)

2.5. Catchment-wide temporal autocorrelation of soil moisture and soil-terrain units

Terrain variables used in the combined soil and terrain stratification were selected by assessing the correlation of each DEM-derived terrain variable to the temporal autocorrelation of soil moisture at 69 out of 106 sites across the catchment, which were regularly measured from 2007 to 2010. We used the Mantel test (Mantel, 1967) to quantify the temporal autocorrelation at 69 monitoring locations, at each depth, with long-term data across the watershed using Euclidean distance between the dates of measurements. The Mantel test generates a statistic called Mantel-r that represents the correlation between two or more distance matrices (Mantel, 1967; McCune and Grace, 2002), which in our case are distance matrices of dates of measurements and soil moisture. We used the Spearman rank correlation for correlating the matrices and tested the significance of these correlations with permutation tests in the *ecodist* library (Goslee and Urban, 2007) of the R statistical software (R Development Core Team, 2013). Distance-based methods are commonly used in ecological literature (*e.g.*, Legendre and Fortin, 1989; Legendre and Legendre, 1998; Uuemaa et al., 2008; Goslee, 2010; Naithani et al., 2014) because they allow incorporation of geographic distances into analyses and do not make assumptions about underlying distributions, as significance is tested based on permutation tests (Goslee, 2010). We replaced geographic distance with temporal distance, particularly to address the uneven temporal gaps (1–2 weeks) in observed data that make it difficult to use the other techniques such as autoregressive models in time series data analysis.

High Mantel-r values indicate a relatively high dependency of soil moisture from previous dates, where the time-series follows a generally consistent pattern of wetting or drying. Mantel-r values that were significant at $p < 0.05$ were then selected for further analysis with terrain variables (58/69 possible Mantel-r values were significant at 10 cm, 59/66 at 20 cm, 53/59 at 40 cm, 40/43 at 80 cm, and 34/36 at 100 cm). To identify predictor terrain variables for use in the combined stratification, the relationship of site-level Mantel-r values at each depth with terrain variables was examined by calculating correlation coefficient for each pair of variables.

As the first step of delineating the combined soil-terrain units, we created a new soil map based upon the high-resolution (1×1 m) LiDAR-derived terrain and depth to bedrock variables (Fig. 2). Terrain has not been used for directly estimating boundaries of soil type in the Shale Hills catchment, and soil type is at least partially defined by landscape position and depth to bedrock in this catchment (Lin et al., 2006). Soil samples taken during the installation of the 106 TDR monitoring sites provided soil type information for each of these locations, but a subset was used for predicted soil mapping in this study, which consists of the minimum number of samples that can represent different soils in the catchment with the same proportion (number of samples per soil type) as the larger dataset. The locations of these 106 TDR sites in the catchment were based on the representation of soil types and dominant landforms (including hillslope, valley floor, and swale), and the chosen subset of 47 sites also offers a balanced representation of each soil type within each dominant landform, *i.e.*, valley floor (Ernest, Blairton), swale (Berks, Rushtown), and hillslope (Weikert).

Selected terrain variables that were highly correlated with the temporal autocorrelation of soil moisture across the catchment were used in a Random Forest ensemble supervised classification tree algorithm (Breiman, 2001) to predict soil types. The Random Forest is a machine-learning algorithm that constructs a large number of regression trees, so that a classification estimate from an ensemble of models can be generated. We generated the soil map by building a supervised classification model with both selected terrain variables (independent variables) and soil type (dependent variable).

A classification tree was built by first sampling 2/3rd of the dataset (out of 47 samples) with an out-of-bag bootstrapping technique, and then a randomly selected subset of predictors was used to fit a decision tree, where a set of rules was assigned to each predictor variable with the objective of minimizing the misclassification of soil type on the

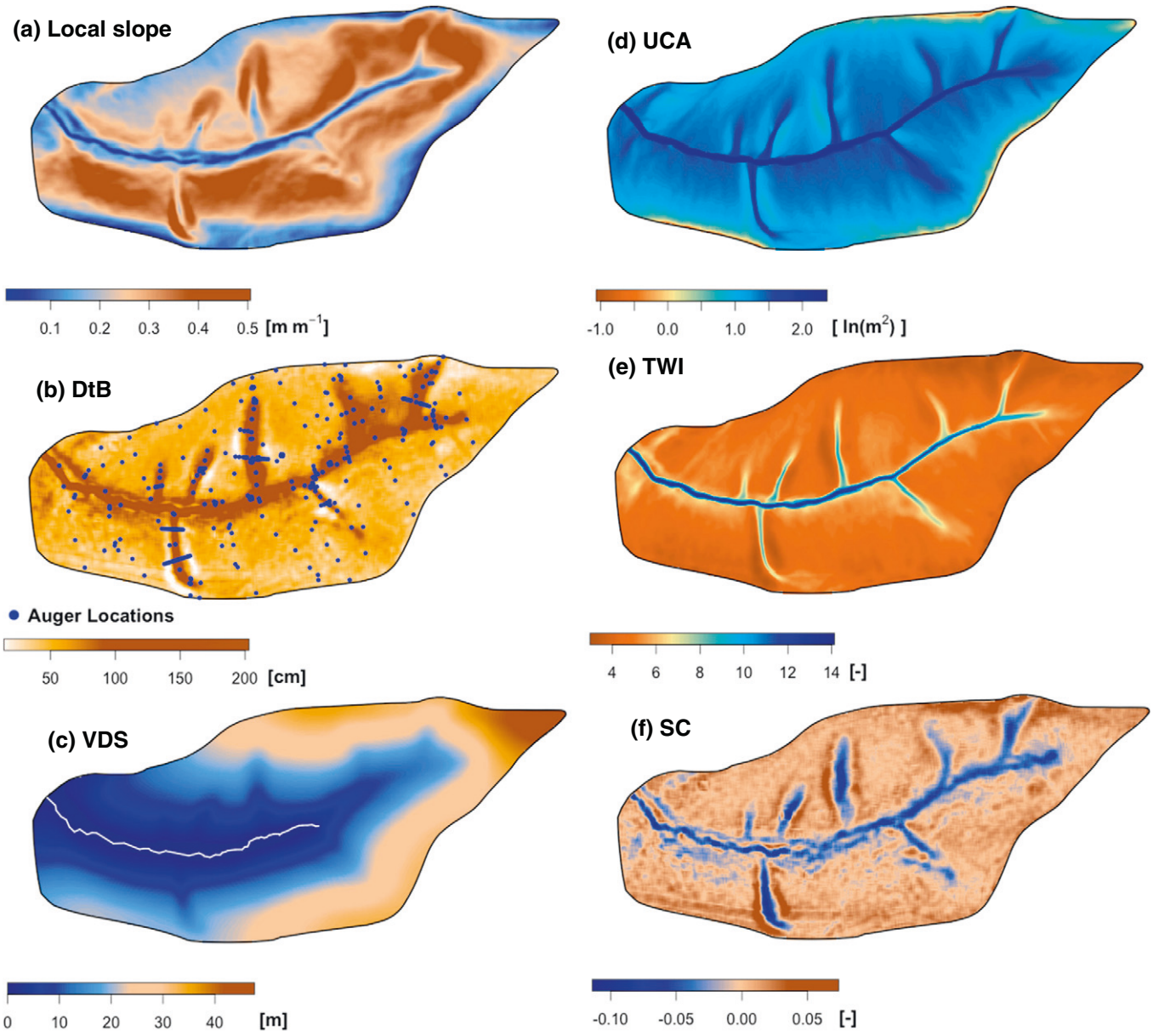

Fig. 2. Maps of terrain attributes derived from the digital elevation model created from 1-m resolution LiDAR: (a) local slope [m m^{-1}], (b) depth to bedrock (DtB) [cm], (c) vertical distance to stream (VDS) [m], (d) natural log-transformed upslope contributing area (UCA) [ln (m^2)], (e) topographic wetness index (TWI) [−], and (f) surface curvature [−].

sub-dataset chosen with bootstrapping. The bootstrapping and classification tree generation was run for 7000 times, so that a large ensemble of classification trees could be generated. Soil type was then assigned to each data point according to what the majority of classification trees in the ensemble chose. A classification error was calculated on the remaining 1/3rd of data not picked with bootstrapping based upon the total number of soil type misclassifications, which was calculated as the proportion of data points misclassified by the algorithm across all ensemble

Table 1
List of key data used in this study.

Section	Variable	Use in This Study
2.2, 2.5, 2.6	Volumetric soil moisture content [cm^3 cm^{-3}] (66 measurement dates; up to 106 locations)	Calculating temporal autocorrelation across the catchment. Validating catchment stratification schemes
2.3	Soil survey samples (289)	Creating detailed soil map from field survey
2.4	Soil depth from auger measurements (318) [m] 1-m resolution LiDAR digital elevation model	Creating depth to bedrock map Creating terrain variables
2.5	Mantel-r for soil moisture content (69 sites; up to 5 different depths) Subset of soil samples from TDR sites (47)	Correlating soil hydrologic dynamics to terrain for variable selection used in stratification Creating detailed soil map with Random Forest and terrain data

Table 2
Summary of the three stratification schemes investigated in this study and related inputs of terrain and soil attributes used in each method.

Stratification method	Terrain input						Soil inputs		Number of units
	UCA[a]	Curvature	TWI[a]	VDS[a]	Slope	Slope class	Field soil samples	DtB[a]	
I. Landform unit	Terrain characterization	Terrain characterization	–	–	Refined summit unit	–	–	–	5
II. Field soil survey	–	–	–	–	–	–	USDA (Order I) field survey	Refine soil boundaries	5
III. Predicted soil map + Slope class	Random forest covariate	Estimate DtB	Estimate DtB	Random forest covariate	Random forest covariate	Final unit stratification	Training for random forest classification	Random forest covariate	7

[a] UCA = Upslope Contributing Area (m^2), TWI = Topographic Wetness Index, VDS = Vertical distance to stream (m), DtB = Depth to Bedrock (cm).

trees. This method makes relatively unbiased estimates of classification error as trees are developed.

Terrain variables used in the Random Forest classification were ranked by importance at the end of the algorithm run using a permutation method, where each predictor variable was randomly permuted, while the rest of the predictors were unchanged, and the classification error was recalculated with the permuted variable. The difference in classification error between the permuted and unchanged variable was calculated for all trees, and the average difference in classification error across all trees defined the 'permutation error difference' measure,

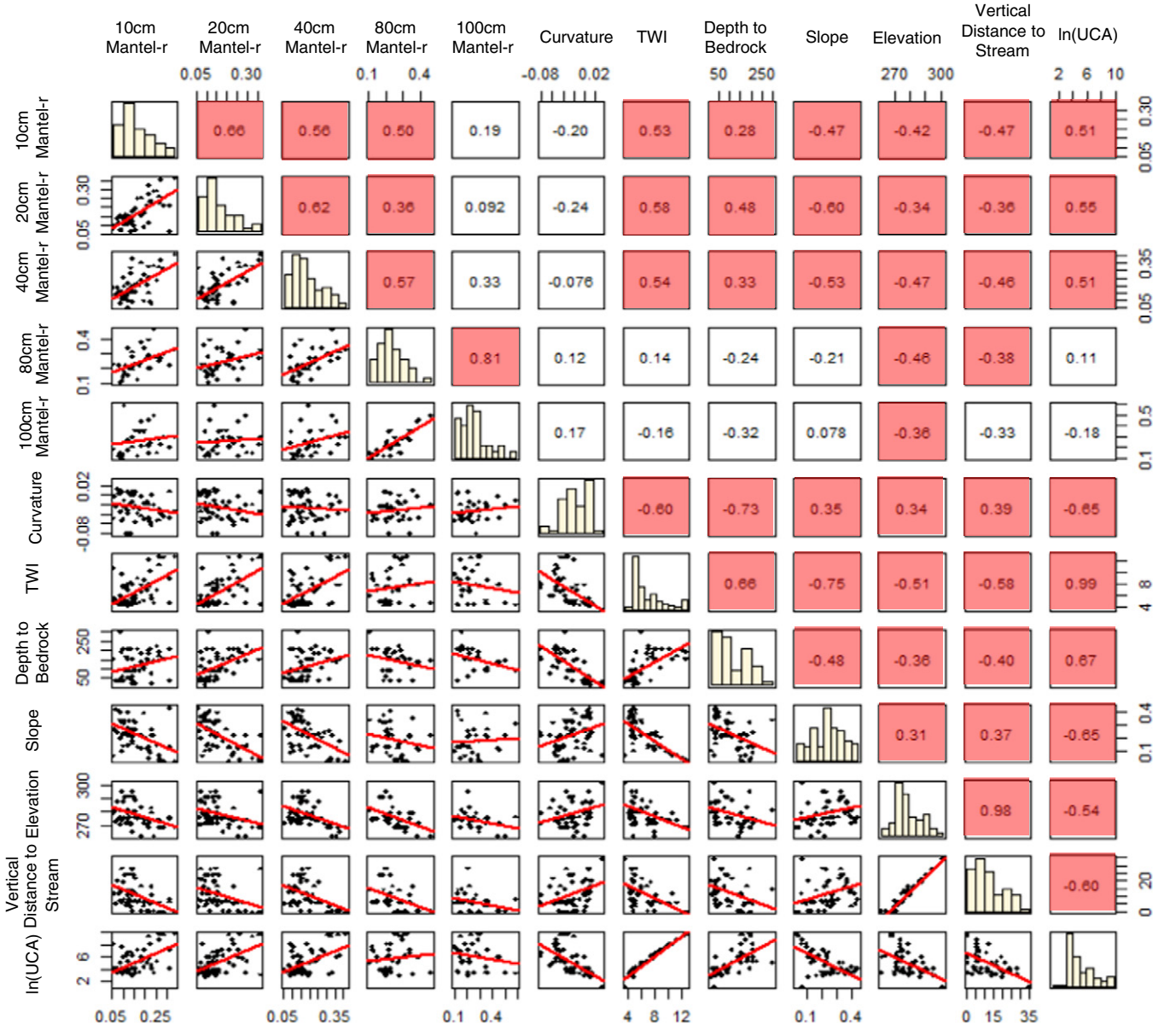

Fig. 3. Correlation matrix showing scatterplots of Mantel correlation coefficient (Mantel-r) of soil moisture at five depths (10–100 cm) and terrain variables from all monitoring sites. Correlation coefficients that are significant at $p < 0.05$ are highlighted in red.

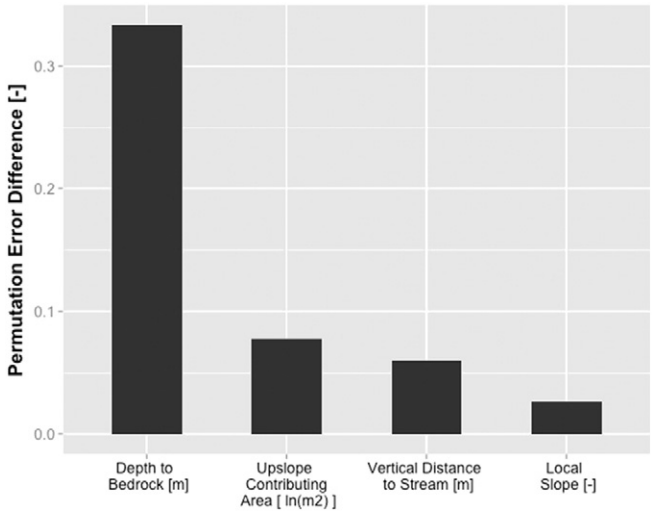

Fig. 4. Bar plots of the difference in classification accuracy within a regression tree forest when each variable is permuted. The higher the permutation error difference, the more important the variable is for predicting soil types in the catchment.

which we used to gauge how much each predictor contributed to model accuracy. Higher permutation error difference values indicate that model classification error is higher if a predictor variable is permuted, and the variable with the highest permutation error difference value is the most important variable to include in the model relative to other predictors.

After generating the predicted soil map with terrain variables, we disaggregated the shallow Weikert soil type on the predicted soil map according to slope classes to generate the final combined soil-terrain unit map. The Weikert soil type covers most of the hillside and contains a relatively large variation of slope values compared to the other soil types in the catchment (Weikert coverage = 78%, slope range = 0.01–0.51 [m m^{-1}]; Berks coverage = 10%, slope range = 0.05–0.48 [m m^{-1}]; Rushtown coverage = 6%, slope range = 0.05–0.40 [m m^{-1}]; Blairton coverage ≤ 1%, slope range = 0.04–0.21 [m m^{-1}]; Ernest coverage = 5%, slope range = 0.01–0.29 [m m^{-1}]). A map of slope classes was created by using the USDA slope class designations: A = 0–3%, B = 3–8%, C = 8–15%, D = 15–25%, and E ≥ 25%. Slope classes A, B, and C were combined into one 0–15% class, since very little area was represented by these classes in this catchment.

2.6. Comparison with classical stratification schemes

The predictive power of soil moisture variability across the catchment was compared between the combined soil-terrain units and two classical stratification schemes, including: (1) landform unit map and (2) field-surveyed soil map. Soil moisture at all 106 sites was predicted by each of these stratification schemes in a linear regression model, where the map unit designations were coded as

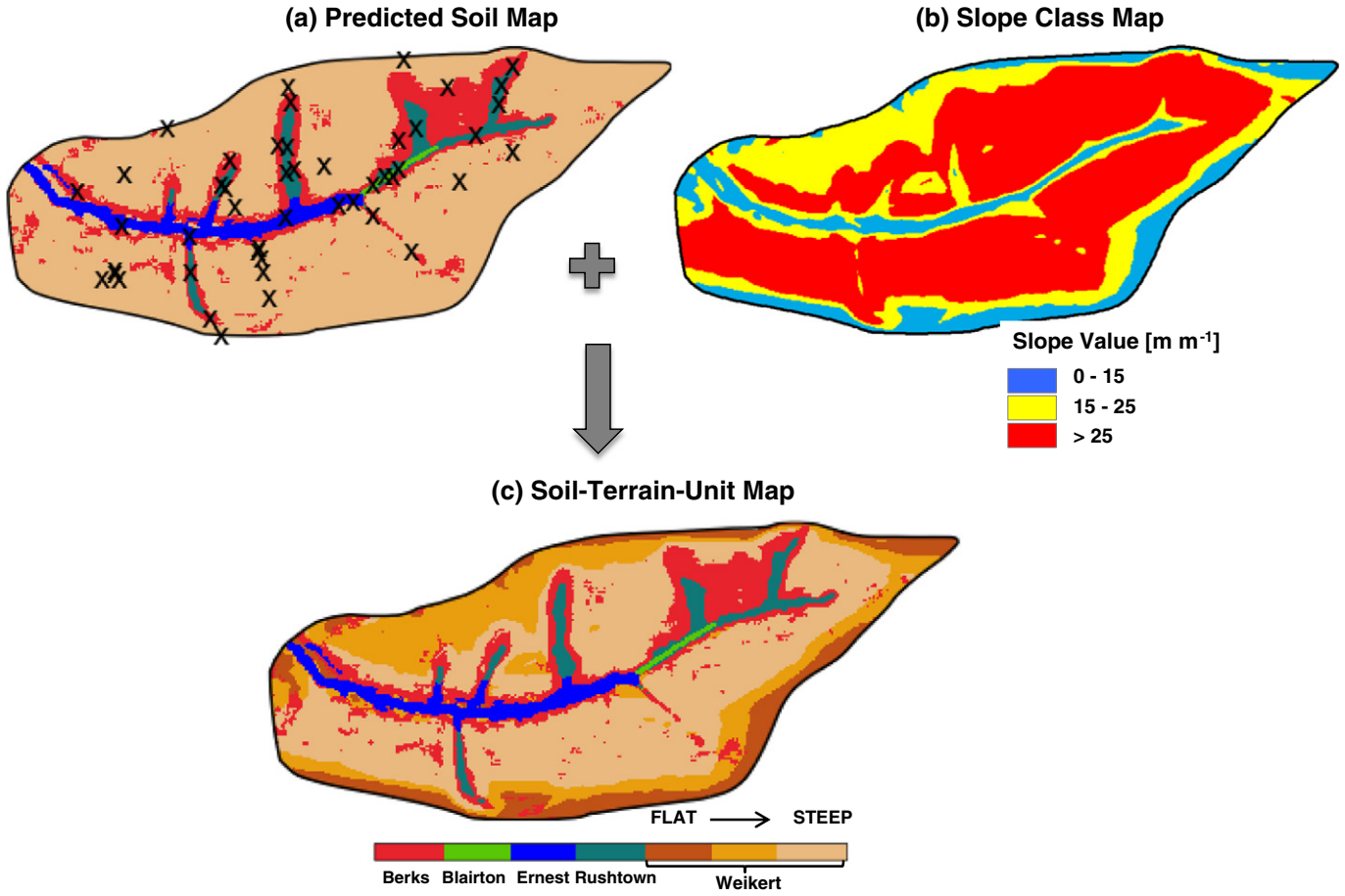

Fig. 5. Sequence of maps used in delineating combined soil-terrain units: (a) predicted soil map based on a Random Forest supervised classification tree algorithm using LiDAR-derived terrain and depth to bedrock as predictors, together with 47 soil samples (marked as 'x' on the map); (b) slope class map; and (c) combined soil-terrain units generated by overlaying the predicted soil map with the slope class map. A total of 7 soil-terrain units are delineated (see the color legend).

unordered factors. The model set-up is the same for each stratification system, where we used a single factor linear regression:

$$\theta_t^{ij} = \beta_o + \sum_{j=1}^{n} \beta_j U_j \quad (1)$$

where θ_t^{ij} is soil moisture content at site i and stratification unit j at measurement date t, n is the total number of units, β_o is the average soil moisture from all sites in a reference unit (arbitrarily chosen in the model), β_j is a regression coefficient for the unit j where site i is located, and U is a 'dummy' coding for a particular unit j. The U coding is '1' if θ^{ij} resides within the same unit as U and '0' otherwise. This regression setup will provide the same model fit as a single factor analysis of variance (ANOVA), and the R^2 is related to the variance of soil moisture within each unit. The difference between a single factor linear regression and an ANOVA is that each category's (*i.e.*, unit's) mean is compared to the overall mean in an ANOVA, while each category's mean is compared to a reference category's mean in a single factor regression. A categorical system with lower overall variance of soil moisture within its units will have a lower R^2 relative to other systems. Separate linear models were developed for each stratification system at each measurement date and for each depth. This allowed the tracking of model performance across time for each depth, since the mean and variation of soil moisture change within each stratification system's units for across different measurement dates.

We used two approaches to analyze the predictive skill of each stratification system's linear model: the Akaike's Information Criterion (AIC) and R^2. The AIC value decreases with low mean model error and increases with the number of parameters or categories used. Since the numbers of map-units across the stratification systems differ, the AIC value is a more balanced performance measure for comparison purposes. We subtracted the AIC value associated with landform units and soil types with the AIC from soil-terrain units to obtain ΔAIC values for all measurement dates and soil depths. If ΔAIC is less than zero, then soil-terrain units do better when predicting soil moisture patterns. We also plotted the R^2 of each linear model over time to assess the raw predictive ability of each stratification system at each depth during the entire measurement period.

3. Results and discussion

In addressing our first objective, we found that the local slope value, UCA, TWI, elevation, VDS and DtB variables related significantly ($p < 0.05$) to Mantel-r values of soil moisture in shallow (10–40 cm) soil depths, while the Mantel-r of soil moisture at deeper depths (80 and 100 cm) showed significant negative relationships with elevation and VDS (Fig. 3). This indicates that soil moisture patterns in deep depths are least organized across time in higher elevations. All of the correlations between the terrain variables and soil moisture autocorrelation at shallow depths consistently suggest that areas with steeper slopes and low upslope contributing area have the lowest temporal structure in shallow soil moisture patterns.

The temporal autocorrelation analysis showed varying degrees to which different terrain variables are correlated to temporal soil moisture autocorrelation over different depths. Just as in Canton et al. (2004), we found a significant relationship between vertical distance to stream channel and temporal soil moisture patterns across all but the deepest soil depth, but our results differ from Canton et al. (2004) in that we found no correlation with surface curvature at any depths but did find significant and high correlations between soil moisture and local slope value. The range of Mantel-r values at different depths reveal that the lowest values exist at 10 cm and steadily increase on average through the lower depths. This reinforces the finding of Takagi and Lin (2011) in their catchment-scale temporal soil moisture variation analysis, where the highest variation of soil moisture over time occurred in shallower depths.

Based on the results from analyzing temporal autocorrelation of soil moisture across the catchment with terrain variables (Fig. 3), we chose local slope (Fig. 2a), UCA (Fig. 2d), VDS (Fig. 2c), and depth to bedrock (Fig. 2b) to predict the distribution of various soil types in the catchment (see Section 2.5). The TWI and elevation variables are highly correlated with UCA and VDS, respectively, which means they do not offer new information for classifying soil type. The area directly around the stream channel (VDS = 0) is important to characterize the Ernest soil type and TWI is a complex variable made up of slope and UCA. Therefore, we chose not to use elevation or TWI in the predictive soil mapping.

The Random Forest analysis uncovered that depth to bedrock is the most important variable for classifying soil types in the Shale Hills catchment, followed by UCA, VDS, and local slope (Fig. 4). Our predicted soil map (Fig. 5a) did a reasonable job in identifying various soil types, with an average classification error of 14.2%. The Weikert (3.9% error) and Ernest (9.1% error) soil types were predicted the best during the Random Forest validation. The most noticeable difference between the predicted soil map (Fig. 5a) and the field surveyed soil map (Fig. 1) was the reduced coverage of the Rushtown soil in favor of the Berks soil in the northeastern part of the catchment. The predicted spatial pattern of the Rushtown soil in this part of the catchment resembled that of a concave hillslope as delineated using the method of Park and van de Giesen (2004) (Fig. 6a). The Berks soil spread farther out from each concave hillslope in the predicted soil map. The Blairton soil spanned a greater distance from where it connected with the Ernest soil eastward along the valley in the predicted soil map, as compared to the field soil map. The slope class map (Fig. 5b) was then overlaid on the predicted soil map (Fig. 5a), which resulted in seven distinct soil-terrain units

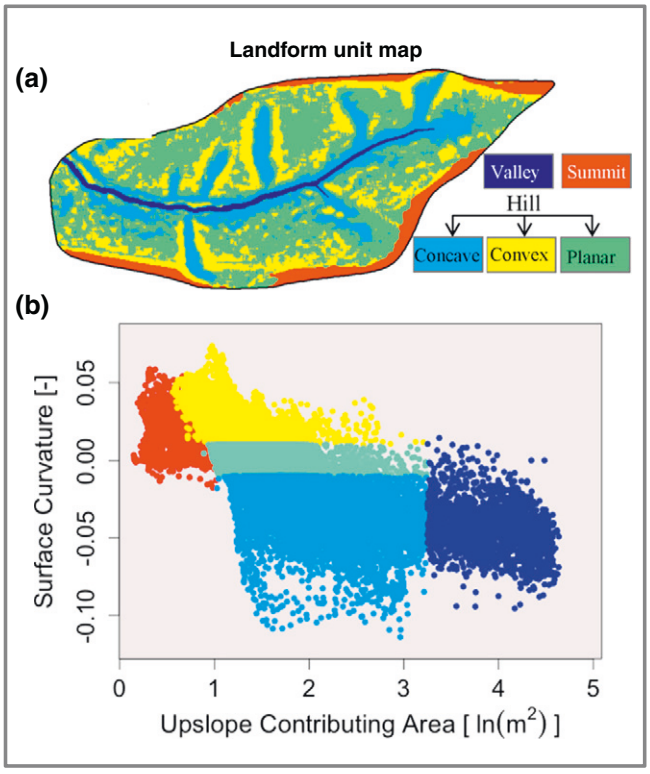

Fig. 6. Landform unit delineated using Park and van de Giesen (2004) method based on surface curvature (Y axis) and log-transformed upslope contributing area (X axis): (a) the resulting map showing 5 landform units across the catchment, and (b) scatterplot with points marked in different colors according to the corresponding landform units in (a).

(Fig. 5c). In comparison, five landform units were generated for the Shale Hills (Fig. 6a) by using the relationship between surface curvature and log-transformed upslope contributing area (Fig. 6b).

When comparing the different catchment stratification schemes for estimating soil moisture content for our second objective, we found that the combined soil-terrain units consistently outperform the landform unit map and the field soil map at most depths, as shown with multiple time-series of R^2 values (Fig. 7). The field soil map did a better job at predicting soil moisture content than the landform unit map across all depths and did equally well as the soil-terrain units at the 10 cm depth over time. The R^2 time-series reveal that predictive power of both the combined soil-terrain units and soil type tends to increase with soil depth but seemed to decrease with depth for the landform unit approach. The total amount of measurements varied for each collection date, but very weak and generally negative correlations between the number of measurements and R^2 exist for all systems. At deeper depths (80–100 cm) soil type and soil-terrain units have very weak positive correlations with the number of measurements and R^2. All of the systems had significant and moderately high positive correlations with catchment averaged moisture and R^2 in the 10 cm depth, but landform units and soil-terrain units had weak but negative correlations with catchment averaged moisture and R^2 in the 40 cm depth (data not shown).

The ΔAIC results shown in Fig. 8 also support the above results. On average, combined soil-terrain units outperform soil type at 20–100 cm depths and outperform landform units over all the monitored depths. From the AIC results, soil-terrain units do better than soil type for most measurement dates at 20–100 cm depths. This could be due to the fact that soil-terrain units are better at differentiating the hillslope by slope class more effectively and as a result characterize soil moisture patterns caused by processes that vary across a slope gradient, such as horizontal, or 'lateral', hydraulic conductivity.

Our stratification analysis revealed that either soil-terrain units or soil type are favorable choices for characterizing soil moisture patterns over landform units in the Shale Hills catchment, and this is supported by both R^2 and AIC model fit diagnostics. In terms of comparing soil-terrain units with soil type, we do acknowledge that R^2 is at least slightly biased in favor of soil-terrain units, since there are two more units (*i.e.*, categories) in the soil-terrain stratification than soil type, but the AIC actually penalizes the soil-terrain units for having two additional regression coefficients.

A further within-stratification analysis of the variance or standard error of soil moisture within each unit over time may reveal the capability of each unit in representing hydrologic dynamics across different catchment wetness conditions. The stratification systems presented in this paper could also be used to parameterize a spatially distributed hydrologic model, and the stratification system that enables such a model to most accurately characterize spatial soil moisture patterns and predict catchment discharge would be best suited for hydrologic modeling applications. An extension of this analysis presented in this paper could also be conducted in other catchments that have an *in situ* soil moisture monitoring network and detailed soil type information.

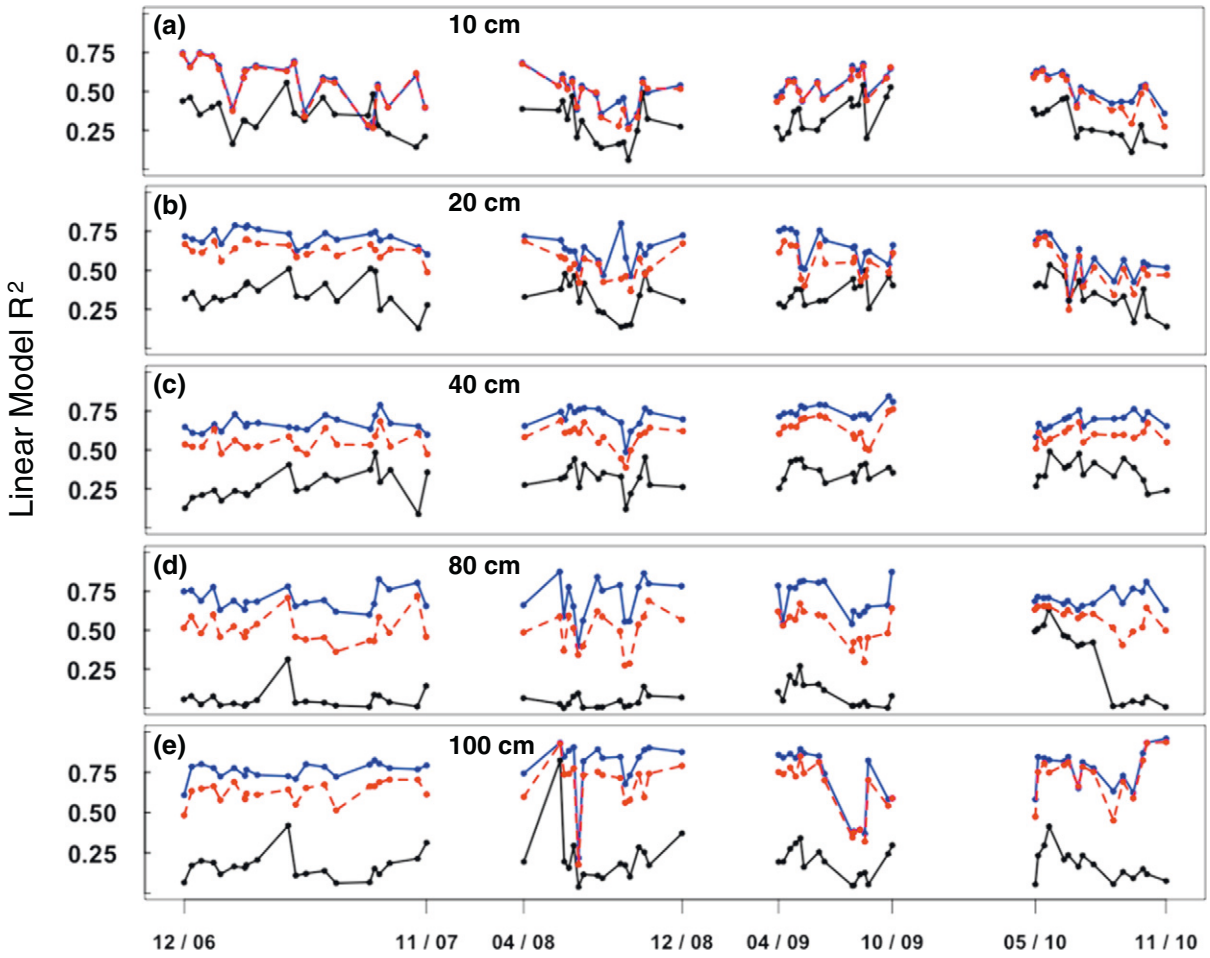

Fig. 7. Comparison of time-series (2006–2010) of R^2 values of generalized linear regression modeling in estimating volumetric soil moisture content [$cm^3\ cm^{-3}$] across the catchment at various depths: (a) 10 cm, (b) 20 cm, (c) 40 cm, (d) 80 cm, and (e) 100 cm, based on three stratification schemes: blue, combined soil-terrain units; red, soil types; and black, landform units.

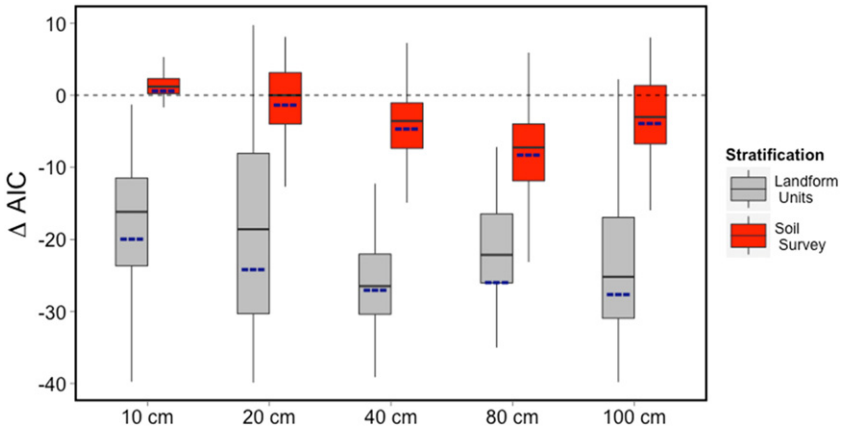

Fig. 8. Boxplots of difference (between soil-terrain unit and other two stratification schemes) in Akaike's Information Criterion (AIC), which are associated with the generalized linear regression models predicting volumetric soil moisture content [$cm^3\ cm^{-3}$] at 10 cm, 20 cm, 40 cm, 80 cm, and 100 cm depths. The ΔAIC is calculated by taking the difference between (1) AIC from regression models that used soil type or landform unit stratification as predictors and (2) AIC from the model using combined soil-terrain units as predictor (*i.e.*, $\Delta AIC_{Landform\ Unit} = AIC_{Soil\text{-}terrain} - AIC_{Landform\ Unit}$; $\Delta AIC_{Soil\ Type} = AIC_{Soil\text{-}terrain} - AIC_{Soil\ Type}$). Combined soil-terrain units perform better than either soil type from field survey or landform unit, with negative ΔAIC (zero ΔAIC indicates no difference between the two models' predictive skill). The blue dashed line indicates the mean ΔAIC value for each boxplot.

4. Conclusion

Integrating soil type and terrain information to stratify the catchment captured soil moisture variation reasonably well in the Shale Hills catchment. From the validation using *in situ* soil moisture data across the catchment, our results showed that soil features provided an added value when used with terrain attributes in stratifying the catchment into areas with similar soil moisture dynamics. We found that depth to bedrock, upslope contributing area, topographic wetness index, and local slope were highly correlated with soil moisture variation at near-surface depths (10, 20, and 40 cm), while elevation and vertical distance to stream were significantly related to the relatively stable patterns of soil moisture found in the deeper depths (80 and 100 cm). The combined soil-terrain attributes were able to predict a soil map similar to that generated from an extensive field survey.

The soil-terrain stratification theme used in this study consistently characterized soil moisture patterns across the catchment at all measured depths more accurately than the existing stratification schemes based on the landform units and even the field soil survey for deeper soils. The field soil survey outperformed the stratification based on the landform units across all soil depths monitored. Given the common approach of using just terrain for catchment stratification, our results suggest that soil types should be considered when stratifying landscapes into units of similar soil hydrologic dynamics.

Acknowledgements

This research was supported in part by the USDA Higher Education Challenge Competitive Grants Program (Grant 2006-38411-17202), the National Science Foundation Hydrologic Sciences Program (grant #EAR-1416881), and the National Science Foundation Critical Zone Observatory Program (#EAR-0725019). This work was conducted in Penn State's Stone Valley Forest, which is supported and managed by the Penn State's Forestland Management Office in the College of Agricultural Sciences. Assistance in the field data collections and maintenance from the Penn State Hydropedology Group is gratefully acknowledged.

References

Band, L.E., Patterson, P., Nemani, R., Running, S.W., 1993. Forest ecosystem processes at the watershed scale: incorporating hillslope hydrology. Agric. For. Meteorol. 63, 93–126.
Beven, K.J., Kirkby, M.J., 1979. A physically based, variable contributing area model of basin hydrology. Hydrol. Sci. Bull. 2, 43–69.
Blöschl, G., Sivapalan, M., 1995. Scale issues in hydrological modelling: a review. Hydrol. Process. 9, 251–290.
Breiman, L., 2001. Random forests. Mach. Learn. 45, 5–32.
Canton, Y., Sole-Benet, A., Domingo, F., 2004. Temporal and spatial patterns of soil moisture in semiarid badlands of SE Spain. J. Hydrol. 285, 199–214.
Conrad, O., Bechtel, B., Bock, M., Dietrich, H., Fischer, E., Gerlitz, L., Wehberg, J., Wichmann, V., Böhner, J., 2015. System for automated geoscientific analyses (SAGA) v. 2.1.4. Geosci. Model Dev. 8, 1991–2007.
R Development Core Team, 2013. R: A Language and Environment for Statistical Computing. R Foundation for Statistical Computing, Vienna, Austria.
Devito, K., Creed, I., Gan, T., Mendoza, C., Petrone, R., Silins, U., Smerdon, B., 2005. A framework for broad-scale classification of hydrologic response units on the boreal plain: is topography the last thing to consider? Hydrol. Process. 19, 1705–1714.
Dooge, J.C.I., 1986. Looking for hydrologic Laws. Water Resour. Res. 22, 46–58.
Gharari, S., Hrachowitz, M., Fenicia, F., Savenije, H.H.G., 2011. Hydrological landscape classification: investigating the performance of HAND based landscape classifications in a central European Meso-scale catchment. Hydrol. Earth Syst. Sci. 15, 3275–3291.
Gomez-Plaza, A., Martinez-Mena, M., Albaladejo, J., Castillo, V.M., 2001. Factors regulating spatial distribution of soil water content in small catchments. J. Hydrol. 253, 211–226.
Goslee, S.C., Urban, D.L., 2007. The ecodist package for dissimilarity-based analysis of ecological data. J. Stat. Softw. 22, 1–19.
Guo, X., Si, B.C., 2008. Characterizing LAI spatial and temporal variability using a wavelet approach. Int. Arch. Photogramm. Remote. Sens. Spat. Inf. Sci. 37, 31–34.
Isaaks, E.H., Srivastava, R.H., 1989. Applied Geostatistics 2. Oxford University Press, New York.
Leavesley, G.H., Stannard, L.G., 1990. Application of remotely sensed data in a distributed-parameter watershed model. Proc. Workshop on Applications of Remote Sensing in Hydrology, pp. 47–68.
Legendre, P., Fortin, M.J., 1989. Spatial pattern and ecological analysis. Plant Ecol. 80, 107–138.
Legendre, P., Legendre, L., 1998. Numerical ecology. Elsevier, Amsterdam.
Lin, H., 2006. Temporal stability of soil moisture spatial pattern and subsurface preferential flow pathways in the Shale Hills catchment. Vadose Zone J. 5, 317–340.
Lin, H., Kogelmann, W., Walker, C., Bruns, M.A., 2006. Soil moisture patterns in a forested catchment: a hydropedological perspective. Geoderma 131, 345–368.
Mantel, N., 1967. The detection of disease clustering and a generalized regression approach. Cancer Res. 27, 209–220.
McCune, B., Grace, J., 2002. Analysis of Ecological Communities. MjM Software, Gleneden Beach, Oregon.
Moore, I.D., Grayson, R.B., Ladson, A.R., 1991. Digital terrain modeling: a review of hydrological, geomorphological, and biological applications. Hydrol. Process. 5, 3–30.
Naithani, K.J., Baldwin, D., Gaines, K.P., Lin, H., Eissenstat, D.M., 2013. Spatial distribution of tree species governs the spatio-temporal interaction of leaf area index and soil moisture across a forested landscape. PLoS One 8.
Naithani, K.J., Ewers, B.E., Adelman, J.D., Siemens, D.H., 2014. Abiotic and biotic controls on local spatial distribution and performance of *Boechera stricta*. Functional Plant Ecology 5, 348.
Odeh, I.O.A., McBratney, A.B., Chittleborough, D.J., 1995. Further results on prediction of soil properties from terrain attributes: heterotopic cokriging and regression kriging. Geoderma 67, 215–226.
Olaya, V., Conrad, O., 2009. Geomorphometry in SAGA. Dev. Soil Sci. 33, 293–308.
Park, S.J., van de Giesen, N., 2004. Soil–landscape delineation to define spatial sampling domains for hillslope hydrology. J. Hydrol. 295, 28–46.
Pauwels, V., Hoeben, R., Verhoest, N.E.C., De Troch, F.P., 2001. The importance of the spatial patterns of remotely sensed soil moisture in the improvement of discharge predictions for small-scale basins through data assimilation. J. Hydrol. 251, 88–102.
Takagi, K., Lin, H.S., 2012. Changing controls of soil moisture spatial organization in the Shale Hills catchment. Geoderma 173, 289–302.

Tarboton, D.G., 1997. A new method for the determination of flow directions and upslope areas in grid digital elevation models. Water Resour. Res. 33, 309–319.
Uuemaa, E., Roosaare, J., Kanal, A., Mander, Ü., 2008. Spatial correlograms of soil cover as an indicator of landscape heterogeneity. Ecol. Indic. 8, 783–794.
Venables, W.N., Ripley, B.D., 2002. Modern Applied Statistics with S. fourth edition. Springer.
Winter, T.C., 2001. The concept of hydrologic landscapes. American Water Resources Association]–>J. Am. Water Resour. Assoc. 37, 335–349.
Yu, X., Duffy, C., Baldwin, D., Lin, H., 2014. The role of macropores and multi-resolution soil survey datasets for distributed surface–subsurface flow modeling. J. Hydrol. 516, 97–106.
Zevenbergen, L.W., Thorne, C.R., 1987. Quantitative analysis of land surface topography. Earth Surf. Process. Landf. 12, 47–56.